Journal of Natural Gas Science and Engineering 2 (2010) 61–68

Contents lists available at ScienceDirect

Journal of Natural Gas Science and Engineering

journal homepage: www.elsevier.com/locate/jngse

# Kinetic studies of the Fischer–Tropsch synthesis over La, Mg and Ca promoted nano–structured iron catalyst

Ali Nakhaei Pour [a,b,*], Mohammad Reza Housaindokht [a], Sayyed Faramarz Tayyari [a], Jamshid Zarkesh [b], Mohammad Reza Alaei [b]

[a] Department of Chemistry, Ferdowsi University of Mashhad, P.O. Box 91775-1436, Mashhad, Iran
[b] Research Institute of Petroleum Industry of National Iranian Oil Company, P.O. Box 18745-4163, Tehran, Iran

ARTICLE INFO

*Article history:*
Received 20 November 2009
Received in revised form
9 February 2010
Accepted 9 February 2010
Available online 26 March 2010

*Keywords:*
Fischer–Tropsch synthesis
Iron-based catalyst
Kinetic parameters
Nano particles
Microemulsion
Promoter

ABSTRACT

The kinetic of the Fischer–Tropsch synthesis (FTS) over nano-structured iron catalyst promoted with Mg, La and Ca, was studied in a continuous spinning basket reactor. Fe/Cu/Si nano-structured catalyst was prepared by co-precipitation in a water-in-oil microemulsion. The results indicated that both the rate constant ($k$) and the adsorption parameter ($b$) in a common two-parameter Fischer–Tropsch rate expression decreased with increasing the catalyst surface basicity. Since decreases in rate constant ($k$) and the adsorption parameter ($b$) affected the FTS rate in reverse direction, the basicity of catalyst surface showed complicated effects on kinetic parameters of FTS reaction. The optimum promoter would be one that its rate constant ($k$) should not be too low and its adsorption parameter ($b$) should not be too high.


## 1. Introduction

Iron-based catalysts are preferred for Fischer–Tropsch synthesis (FTS) utilizing synthesis gas derived from coal or biomass because of the excellent activity for the water–gas-shift (WGS) reaction, which allows using a synthesis gas with a low $H_2/CO$ ratio directly without an upstream shift-step (Anderson, 1984; Dry, 1981; Bartholomew, 1991; Mills, 1988). The FTS and WGS reactions are as following:

$$CO + (1 + n/2)H_2 \rightarrow CH_n + H_2O \quad (1)$$

$$CO + H_2O \leftrightarrow CO_2 + H_2 \quad (2)$$

Where $n$ is the average H/C ratio of the produced hydrocarbons. Recent studies showed that nano-sized iron particles played an essential role to achieve high FTS activity (Hayashi et al., 2002; Li et al., 1994; Herranz et al., 2006; Eriksson et al., 2004; Schwuger et al., 1995; Liu et al., 2000; Nakhaei Pour et al., 2009, in press). In recent years, it has been generalized using microemulsions for synthesize of nano particles with controlled size, which display a homogeneous distribution of both elements throughout the solid (Herranz et al., 2006; Eriksson et al., 2004). A prepared microemulsion catalyst, which is optically transparent and has thermodynamically stable dispersion of water phase into an organic phase, is stabilized by a surfactant (Schwuger et al., 1995). The different species (oxide precursors) in microemulsion systems are homogeneously mixed within the micelles, as a result, the internal interaction between catalyst and promoters in comparison with the general catalyst preparation method would be better. Therefore rendering the solids displayed high internal homogeneity and optimal interaction between the constituents (Herranz et al., 2006; Eriksson et al., 2004). Herranz et al. (2006), prepared supported iron-based Fischer–Tropsch catalysts by microemulsion, reported high activity and marked selectivity to oxygenate (Herranz et al., 2006). Previously we studied the effects of nano-size iron particles on catalyst structure, surface area, reduction and carburization, textural properties, and activity behavior of precipitated Fe/Cu/La catalyst in a fixed bed reactor (Nakhaei Pour et al., 2009, in press).

Typically, iron-based catalysts often contain small amounts of potassium and/or some other metals such as manganese,

* Corresponding author. Research Institute of Petroleum Industry of National Iranian Oil Company, P.O. Box 18745-4163, Tehran, Iran. Tel./fax: +98 21 44739716.
*E-mail addresses:* nakhaeipoura@ripi.ir, nakhaeipoura@yahoo.com (A. Nakhaei Pour).

1875-5100/$ – see front matter © 2010 Elsevier B.V. All rights reserved.
doi:10.1016/j.jngse.2010.02.004

calcium, zinc, copper and magnesium to promote catalyst activity and selectivity (Nakhaei Pour et al., 2008a, 2008b, 2008c; Yang et al., 2006; Li et al., 2001; Tao et al., 2006; Hoc et al., 2002; Zhang et al., 2006; Yang et al., 2004; Raje et al., 1998; Luo and Davis, 2003; Bukur et al., 2001; Guczi and Lázár, 1991; Gallegos et al., 1996). High basicity property of potassium influences on the adsorption of reactants (CO and $H_2$) on the catalyst surface, which improved FTS catalyst activity that leads to increase in the selectivity to olefins, suppression of the methane formation and shift in selectivity to higher molecular weight products (Yang et al., 2004; Raje et al., 1998). Luo and Davis (2003) compared group II alkali-earth metal-promoted iron-based catalysts with potassium-promoted and unpromoted catalysts under medium pressure conditions. They concluded that the promoted catalysts with MgO and CaO have lower FTS and WGS activity than the potassium-promoted iron catalyst, but they have higher activity and chain growth factor than unpromoted catalysts. Bukur et al., 2001 reported that the incorporation of CaO promoter into a precipitated $Fe/Cu/K/SiO_2$ catalyst has a negative effect on the catalytic activity. Guczi and Lázár (1991) found CaO as an inert promoter in supported Fe/MgO catalyst while it increased metal dispersion. Gallegos et al. (1996) investigated the $Fe/SiO_2$–MgO catalysts for FTS reaction. Their experimental results showed that the rate of total hydrocarbon formation increases with MgO. The optimal content of MgO increased the selectivity to the olefins and suppressed formation of methane. Effects of Ca, Mg and La promoters on physico-chemical properties, catalytic activity and selectivity during FTS performance have been studied in our previous work (Nakhaei Pour et al., 2008b). The addition of the promoters increased the catalyst surface basicity and catalytic activity (FTS and WGS) in the order Ca > Mg > La > unpromoted.

The kinetics of the Fischer–Tropsch synthesis have been studied extensively to describe the reaction rate using a power law rate equation or an equation based on certain mechanistic assumptions (Vannice, 1976; Huff and Satterfield, 1984; Zimmerman and Bukur, 1990; Van der Laan and Beenackers, 1999; Bell, 1981; Anderson, 1956). An overview of rate equations for iron catalysts is given by Vannice (1976), Huff and Satterfield (1984), Zimmerman and Bukur (1990), and Van der Laan and Beenackers (1999). Literature reviews indicate a few reports on the effects of the alkali promotation on the kinetic parameters of the Fischer–Tropsch Synthesis in detail. Raje et al. (1998) studied the effect of the potassium loading on the kinetic parameters, changes in these parameters and catalyst activity.

The effect of Ca, Mg and La promoters on kinetic parameters of FTS of nano-structured $Fe/Cu/SiO_2$ catalysts has been determined in this study. By analyzing the results of increasing the catalyst surface basicity we discern the reasons of changes in catalyst activity and kinetic parameters.

## 2. Experimental

### 2.1. Catalyst preparation

A Fe–Cu–Si nano-structured catalyst was prepared by co-precipitation in a water-in-oil microemulsion procedure as described previously. The crystal size of the nano catalyst was 20 nm, as determined in our previous work (Nakhaei Pour et al., 2009, in press). The Ca, Mg and La promoters were added by incipient wetness impregnation. Final catalyst compositions were designed in terms of the atomic ratio as 100Fe/5.64Cu/2La, 2Ca or 2Mg/19Si that were verified by an inductively coupled plasma (ICP) AES system.

### 2.2. Catalytic performance

Steady-state FTS reaction rates and selectivities were measured in a continuous spinning basket reactor (stainless steel, $H = 0.122$ m, $D_0 = 0.052$ m, $D_i = 0.046$ m) with temperature controllers (WEST series 3800). A J-type movable thermocouple made it possible to monitor the bed temperature axially, which was within 0.5 K of the average bed temperature. The reactor system also included a stainless steel cold trap at ambient temperature located before the gas chromatograph sampling valve. Incondensable gases were passed through sampling valve into an online gas chromatograph continuously then vent through a soap-film bubble meter. Two separate Brooks 5850 mass flow controllers were used to add the desired flow rate of $H_2$ and CO to admixing vessel, preceded by palladium and molecular sieve traps to remove metal carbonyls and water before entering to the reactor. A compact pressure controller was used to control the pressure. The flow rate of tail gas is measured by a wet test gas meter.

Blank experiments show that the spinning basket reactor charged with inert silica sand without the catalyst has no conversion of syngas. The weight of the catalyst loaded is 2.5 g and diluted by 10 $cm^3$ inert silica sand with the same mesh size range. The catalyst samples were activated by a 5% (v/v) $H_2/N_2$ gas mixture with space velocity equal to 15.1 nl $h^{-1}$ $g_{Fe}^{-1}$ at 0.1 Mpa and 1800 rpm. The reactor temperature increased to 673 K with a heating rate of 5 K/min, maintained for 1 h at this temperature, and then let it to reduce to 543 K spontaneously. The activation is followed by the synthesis gas stream with $H_2/CO = 1$ and space velocity equal to 3.07 nl $h^{-1}$ $g_{Fe}^{-1}$ for 24 h in 0.1 MPa and 543 K. After catalyst reduction, synthesis gas was fed to the reactor at conditions operated at 563 K, 1.7 MPa, ($H_2$/CO) feed = 1 and a space velocity equal to 10.4 nl $h^{-1}$ $g_{Fe}^{-1}$. A stabilization period of 15 h is conducted under the reaction conditions, and then the kinetics measurement is carried out.

During kinetics measurement runs, temperature varied between 543 and 593 K, pressure was 1.7 MPa, ($H_2$/CO) feed = 1, stirring speeds is 1800 rpm and the space velocity of the synthesis gas varied between 3.5 and 28.7 nl $h^{-1}$ $g_{Fe}^{-1}$. Conversion of carbon monoxide and hydrogen, and the formation of various products were measured with a period of 12 h at each space velocity. Periodically during the run, the catalyst activity was measured at "standard" condition (563 K, 1.7 MPa, $H_2$/CO ratio = 1 and space velocity 10.4 nl $h^{-1}$ $g_{Fe}^{-1}$) repeatedly and was compared to check the catalyst deactivation. The water partial pressure was determined by collecting the water in the trap, separating it from the oil, and weighing. The weight of water was converted to partial pressure in the reactor based upon the ideal gas law.

The external mass transfer limitation is investigated by comparing the CO conversions under different stirring speeds of the reactor. The corresponding stirring speed should ensure that the experimental data measured are in the kinetically limited regime. In our experiments, all the experiments are carried out at 1800 rpm, which is safe to eliminate the external mass transfer limitations for all kinetic conditions.

The products were analyzed by means of three gas chromatographs, a Shimadzu 4C gas chromatograph equipped with two subsequent connected packed columns: Porapak Q and Molecular Sieve 5A, and a thermal conductivity detector (TCD) with Ar as carrier gas, which was used as a carrier gas for hydrogen analysis. A Varian CP 3800 with a chromosorb column and a thermal conductivity detector (TCD) were used for CO, $CO_2$, $CH_4$, and other non-condensable gases. A Varian CP 3800 with a Petrocol$^{Tm}$ DH100 fused silica capillary column and a flame ionization detector (FID) was used for organic liquid products. So, a complete product distribution could be provided.

## 3. Results

The FTS reaction rate for iron catalysts commonly increases with $H_2$ partial pressure and decreases with water partial pressure. Anderson (1956) proposed an empirical rate equation with water inhibition:

$$-r_{CO+H_2} = \frac{kP_{CO}P_{H_2}}{P_{CO} + aP_{H_2O}} \quad (3)$$

Where, $k$ and $a$ are kinetic constant and adsorption parameter, respectively. Huff and Satterfield (1984) observed a linear decrease in the adsorption parameter $a$ in Eq. (3) with hydrogen pressure on a fused iron catalyst and incorporated this effect by modifying Eq. (3) to

$$-r_{CO+H_2} = \frac{kP_{CO}P^2}{P_{CO}P_{H_2} + bP_{H_2O}} \quad (4)$$

Note that $b$ in Eq. (4) equals $a/P_{H_2}$ in Eq. (3). Based on this rate expression, changes in catalyst FTS activity may be due to changes in: (i) rate constant ($k$), (ii) adsorption parameter ($b$), and (iii) partial pressure of water. The reaction rate expression given in Eq. (4) is linearized by rearrangement as:

$$\frac{P_{H_2}}{-r_{CO+H_2}} = \frac{1}{k} + \frac{b}{k}\frac{P_{H_2O}}{P_{CO}P_{H_2}} \quad (5)$$

Hence a plot of $P_{H_2}/-r_{CO+H_2}$ vs.$P_{H_2O}/P_{CO}P_{H_2}$ should give a straight line with intercept of $1/k$ and slope of $b/k$. The rate of syngas consumption was fitted into the linearized kinetic model (Eq. (5)), in order to study the effects of promoters and the catalyst surface basicity on the kinetic parameters. These data for the La, Ca and Mg promoters at various temperatures are plotted in Figs. 1–3. They indicate that the results for carbon monoxide conversions of less than 60% lie on a straight line but the results for higher carbon monoxide conversions deviate substantially for all the catalysts because the FTS reaction highly depends on the hydrogen formed by the WGS as the carbon monoxide conversion increases. Thus, the overall FTS reaction rate is highly affected by the rate/extent of the WGS reaction at high FTS conversions. The FTS reaction rate is unaffected by the WGS reaction only at lower conversions (Raje et al., 1998). In order to estimate the FTS reaction rate, regression lines in Figs. 1–4 were drawn for the data at carbon monoxide conversions below 60%. Obtained data from these regression lines primarily just correspond to the FTS reaction.

The calculated rate constant ($k$) and adsorption parameter ($b$) at various temperatures for La, Ca and Mg promoters are listed in Table 1. These data showed that the rate constant ($k$) of FTS reaction was decreased by increasing the basicity of the catalyst in the order Ca > Mg > La. This means that the FTS rate decreased by increasing the catalyst surface basicity (Nakhaei Pour et al., 2008b). The activation energy of FTS reaction for these promoted catalysts can be determined from calculated rate constant ($k$), using the Arrhenius equation that directly introduced into the kinetic parameters:

$$k = k_\infty \exp\left(\frac{-E_A}{RT}\right) \quad (6)$$

Hence, a plot of $\ln(k)$ vs. $1/T$ should give a straight line with slope of $-E_A/R$. The logarithm of the rate constant ($k$) is plotted in Fig. 4 as a function of reciprocal temperature for promoted catalysts with Ca, Mg and La. From the slope of the curves in Fig. 4, the activation energy of Ca, Mg and La promoters determined 92, 78 and 70 kJ/mol, respectively that are listed in Table 1. It means that by raising the catalyst surface basicity, the activation energy of FTS reaction increased and FTS reaction rate decreased consequently.

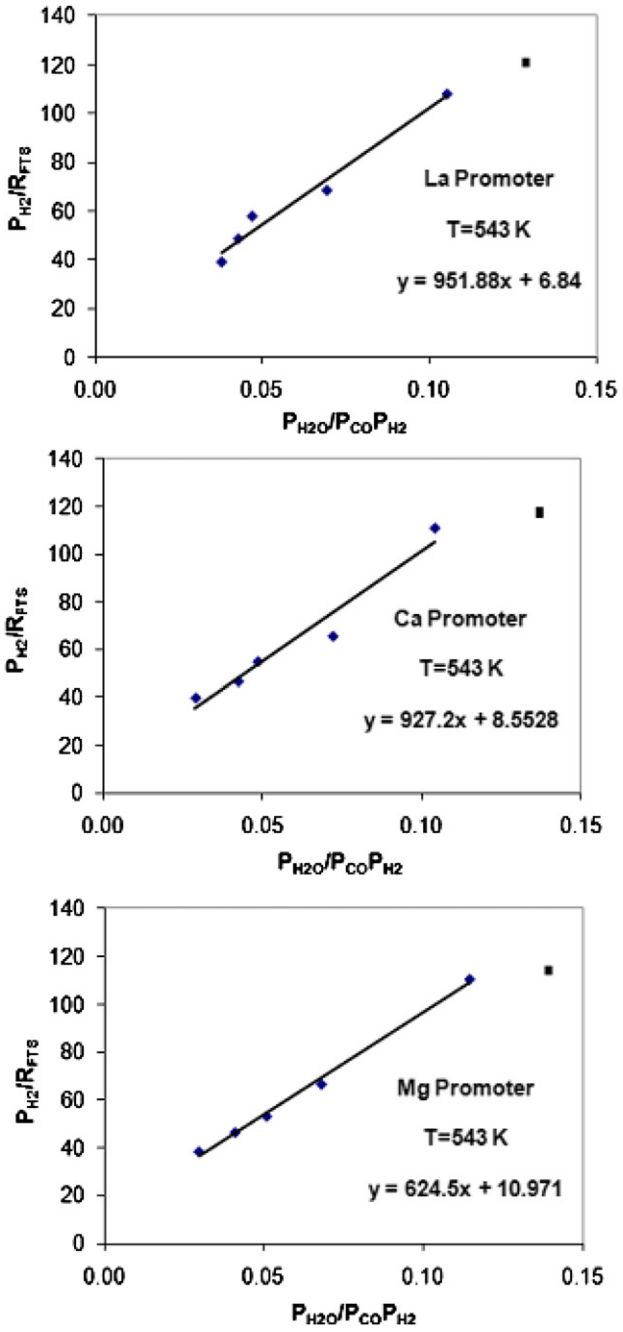


**Fig. 1.** Plots of the calculated $P_{H_2}/R_{FTS}$ (bar h $g_{Fe}$ $mol^{-1}$) vs. $P_{H_2O}/P_{CO}\cdot P_{H_2}$ ($bar^{-1}$) according to linerized Huff and Satterfield FTS rate equation (Eq. (8)) (Raje et al., 1998) for La, Mg and Ca promoters at $T = 543$ K.

Table 1 also shown comparison of the adsorption parameter ($b$) for the different kind of promoters. The adsorption parameter ($b$) in kinetic model proposed by Huff et al. (Huff and Satterfield, 1984) was shown to be given by $b = K_{H_2O}/K_{CO}$, where $K_{H_2O}$ and $K_{CO}$ are adsorption equilibrium constants for water and carbon monoxide, respectively. As shown in Table 1, with increasing the catalyst surface basicity in the order Ca > Mg > La, the adsorption parameter $b$ was decreased. Thus, a decrease in the adsorption parameter ($b$) can be due to a decrease in the adsorption equilibrium constant for water and/or an increase in the adsorption equilibrium constant for carbon monoxide. Previous studies have shown that the alkali promoters caused an increase in the adsorption equilibrium

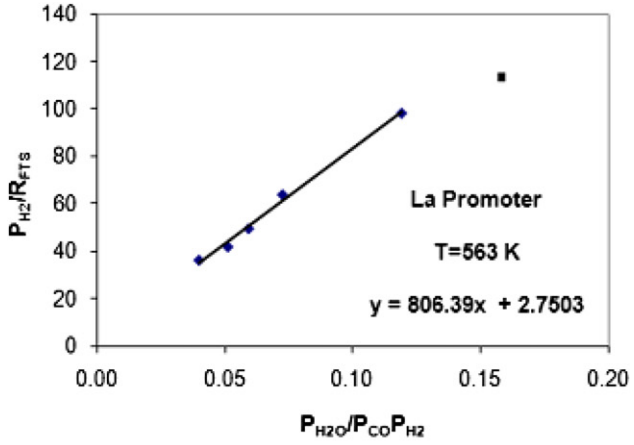


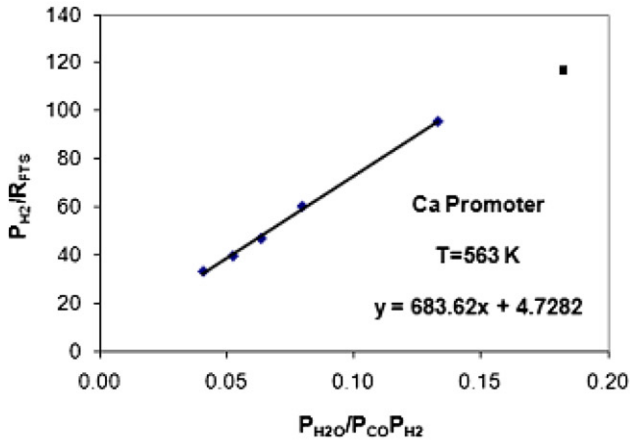


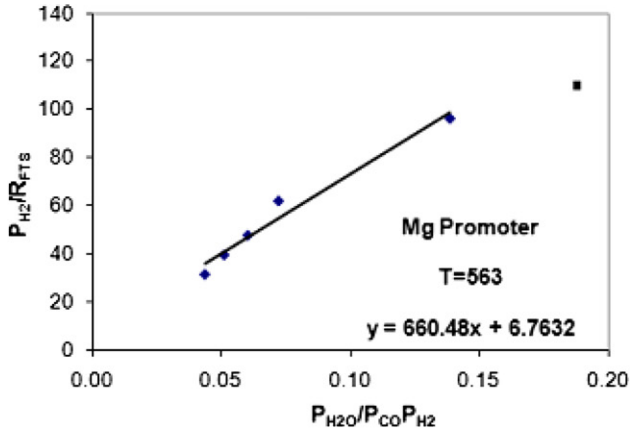


**Fig. 2.** Plots of the calculated $P_{H_2}/R_{FTS}$ (bar h $g_{Fe}$ $mol^{-1}$) vs. $P_{H_2O}/P_{CO}\cdot P_{H_2}$ ($bar^{-1}$) according to linerized Huff and Satterfield FTS rate equation (Eq. (8)) (Raje et al., 1998) for La, Mg and Ca promoters at $T = 563$ K.

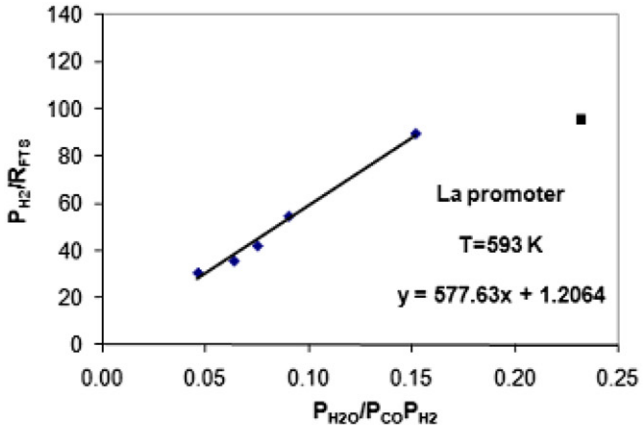


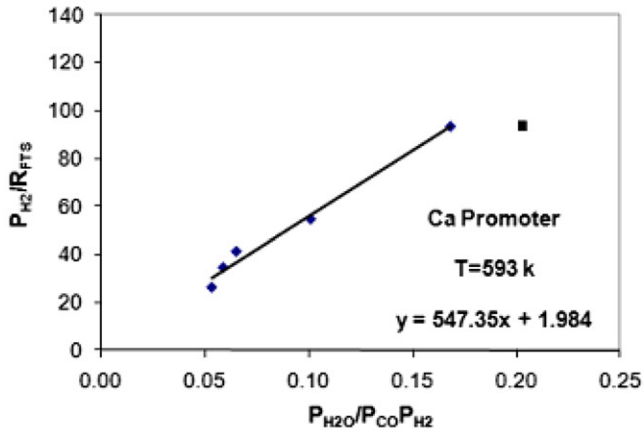


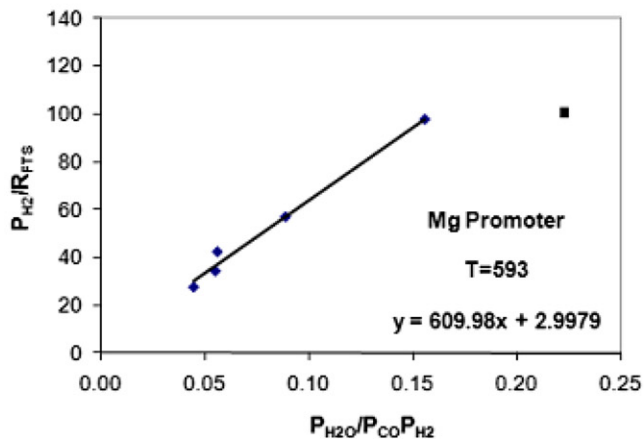


**Fig. 3.** Plots of the calculated $P_{H_2}/R_{FTS}$ (bar h $g_{Fe}$ $mol^{-1}$) vs. $P_{H_2O}/P_{CO}\cdot P_{H_2}$ ($bar^{-1}$) according to linerized Huff and Satterfield FTS rate equation (Eq. (8)) (Raje et al., 1998) for La, Mg and Ca promoters at $T = 593$ K.

constant for carbon monoxide (Dictor and Bell, 1986; Arakawa and Bell, 1983; Dry et al., 1969; Benziger and Madix, 1980). The observed decrease in the adsorption parameter ($b$) with increasing the basicity of promoters is consistent with the results of these studies. A decrease in the adsorption parameter ($b$) with promoters implies an increase in the FTS rate with catalyst surface basicity. Thus, optimum promoter would be one that its rate constant ($k$) should not be too low and its adsorption parameter ($b$) should not be too high.

The apparent heat of adsorption for the combined term $b$ is:

$$-\Delta H_{ads,b} = \Delta H_{ads,CO} - \Delta H_{ads,H_2O} \tag{7}$$

Adsorption enthalpy $\Delta H_{ads,b}$ can be determined with adsorption parameter $b$ via

$$b = b_\infty \exp\left(\frac{-\Delta H_{ads,b}}{RT}\right) \tag{8}$$

Hence, a plot of ln ($b$) vs. $1/T$ should give a straight line with slope of $-\Delta H_{ads,b}/R$. The logarithm of the parameter $b$ is plotted in Fig. 5 as a function of reciprocal temperature for catalysts promoted with Ca,

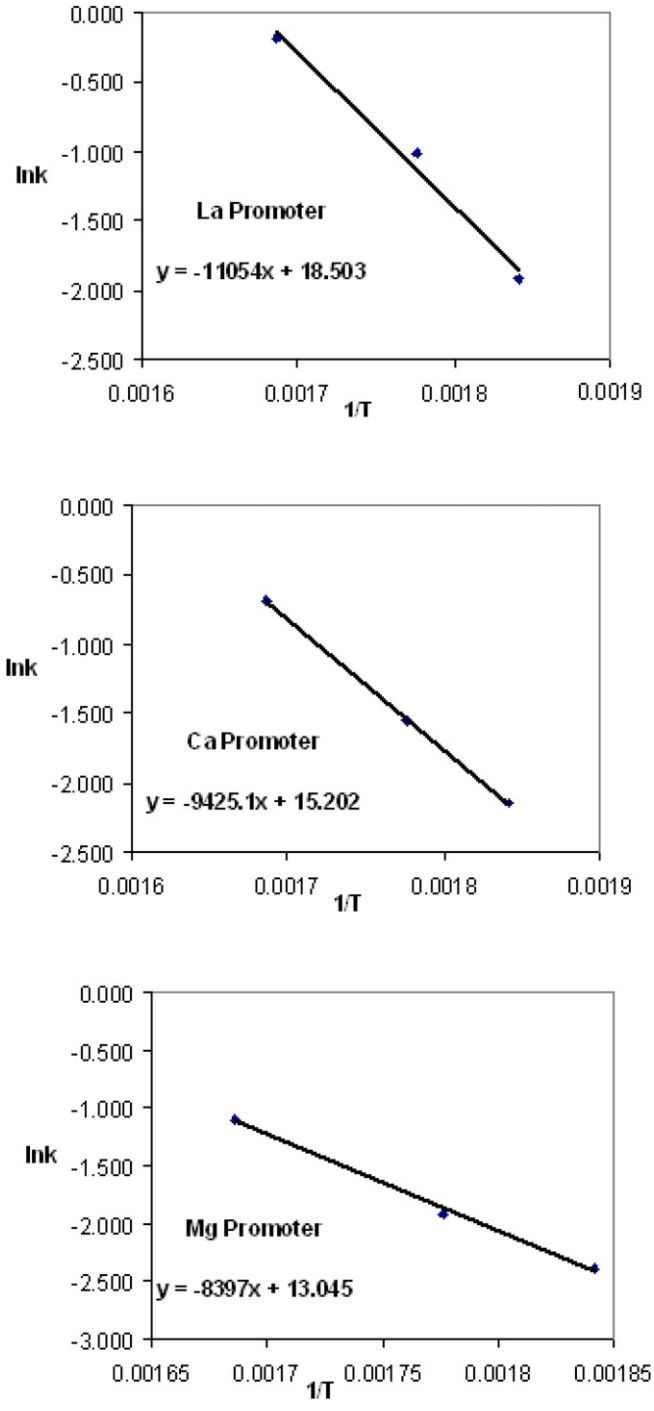


**Fig. 4.** Plots of the calculated FTS rate constant ($k$) (mol $h^{-1}$ $g_{Fe}$ $bar^{-1}$) vs. reciprocal temperature ($K^{-1}$) as a function of La, Ca and Mg promoters.

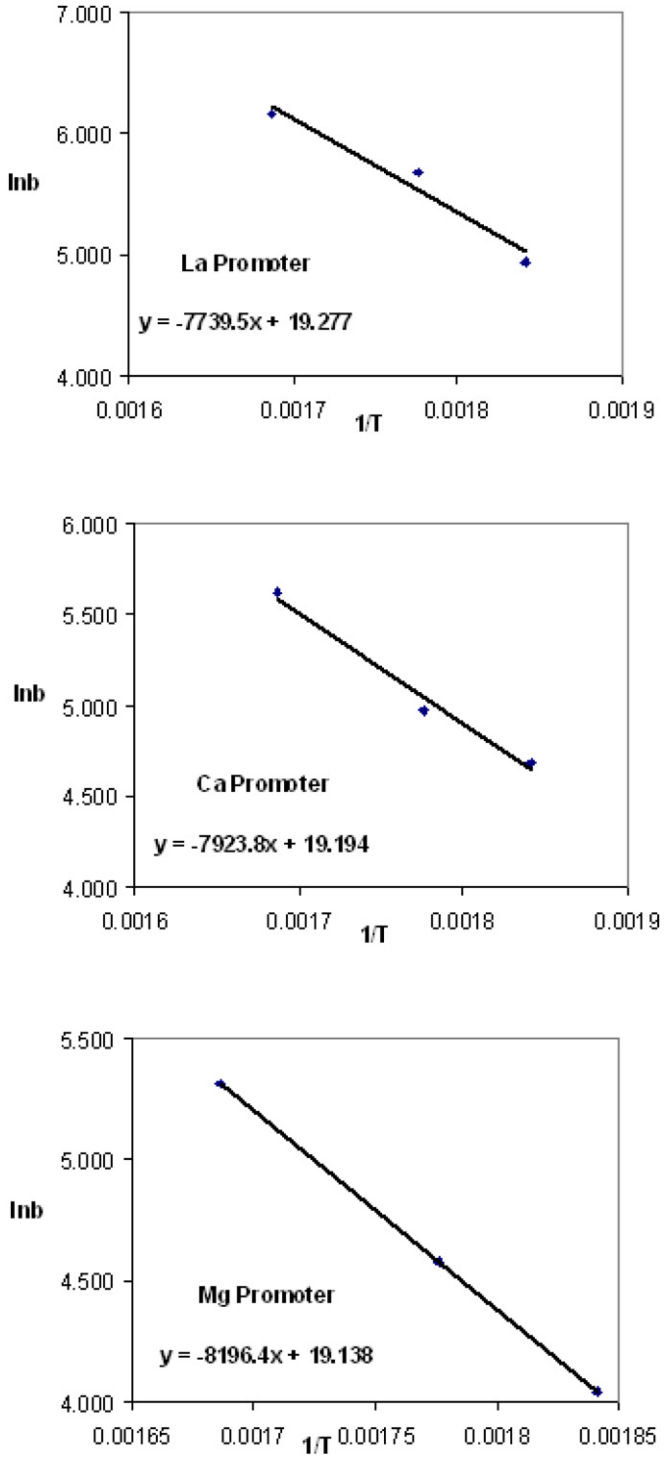


**Fig. 5.** Plots of the calculated FTS adsorption parameter ($b$) vs. reciprocal temperature ($K^{-1}$) as a function of La, Ca and Mg promoters.

**Table 1**
Kinetic parameters of promoted catalysts.

| Catalyst | $k$ (mol $h^{-1}$ $g_{Fe}^{-1}$ $bar^{-1}$) | | | $b$ (bar) | | | $E_A$ | $\Delta H$ |
|---|---|---|---|---|---|---|---|---|
| | 543 K | 563 K | 593 K | 543 K | 563 K | 593 K | kJ | kJ |
| Fe/Cu/La/Si | 0.15 | 0.36 | 0.83 | 139 | 293 | 474 | 70 | 69 |
| Fe/Cu/Mg /Si | 0.12 | 0.21 | 0.51 | 108 | 145 | 276 | 78 | 66 |
| Fe/Cu/Ca /Si | 0.09 | 0.15 | 0.33 | 78 | 98 | 203 | 92 | 64 |

Mg and La. From the slope of the curves in Fig. 5, the heats of adsorption ($b$) of Ca, Mg and La promoters are determined 64, 66 and 69 kJ/mol, respectively. It means that, the heats of adsorption for water, which are 64, 66 and 69 kJ/mol are larger than those values for carbon monoxide adsorption for these promoters. These results show that by raising the catalyst surface basicity, the heats of adsorption of carbon monoxide in comparison with water increased significantly.

## 4. Discussion

By 1926, Fischer and Tropsch (1926) suggested that the carbide mechanism whereby carbides that were formed from the synthesis gas were then hydrogenated to methylene groups. These methylene groups could polymerize to form hydrocarbon chains that desorbs from the surface as saturated and unsaturated hydrocarbons as shown in Scheme 1.

However, the formation of oxygenates is hardly feasible via the $CH_2$ insertion mechanism. Therefore, oxygenates are assumed to be formed via the CO insertion mechanism. Near the end of the World War II, Paul Emmett joined the Mellon Institution and studied the FTS. He was fortunate that this work on the Manhattan Project made him aware of the use of radioisotope and provided connection at Oak Ridge so that he could obtain some of initial supplies of $^{14}C$. Using $^{14}C$ he was able to show that the hydrogenation of the iron carbide labeled with $^{14}C$ was not the dominant source of the hydrocarbons and thereby requiring their formation by the reaction of CO with $H_2$ (Podgurski et al., 1950). These results supported his earlier calculation showing that the hydrogenation of iron carbide to form hydrocarbons was not the reaction pathway (Kummer et al., 1948). The work of Emmett et al., combined with the work at the US Bureau of Mines, led to wide spread acceptance of the oxygenate reaction mechanism for FTS (Storch et al., 1951). The simple offered oxygenate reaction mechanism is shown in Scheme 2.

With the advent of the surface science instrumentation, the view shifted from the oxygenate to once again the carbide mechanism from 1970 (Davis, 2009). A reason for this was the observations made using surface science instruments that show essentially the absence of oxygen on the catalyst surface but an abundance of carbon. This led to the view that it was a surface, or near surface, metal carbide that was the initial surface species in the formation of carbenes.

In general, for iron catalysts, the FT reaction rate increases with $H_2$ partial pressure and decreases with partial pressure of water. The Langmuir–Hinshelwood–Hougen–Watson (LHHW) type of kinetic rate expressions for iron catalysts are all based on the formation of the $C_1$ species as the rate-determining step in the consumption of synthesis gas. $C_1$ species on the surface initiates polymerization; the product distribution is determined by relative rates of chain growth and termination. However, the carbide or oxygenate theories and kinetic information available provide guidelines to assist in developing rate expressions. Huff and Satterfield (1984) used the carbide and oxygenate theories to obtain Eq. (4), which these two approach lead to the same formula.

In oxygenate mechanism, the rate constant ($k$) is related to the rate-determining step consists of the final hydrogenation of the acidic CO–$H_2$ complex.

$$CO{-}H_2^* + H_2 \rightarrow CH_2^* + H_2O \tag{10}$$

Also in carbide theory, CO dissociates on the surface and adsorbed carbon reacts with hydrogen in the rate-determining step. Constant ($k$) is related to the following step.

$$C^* + H_2 \rightarrow CH_2^* \tag{11}$$

As shown in Fig. 5, the rate of this reaction decreases while the catalyst surface basicity increases. Nevertheless, the catalyst surface basicity has no effect on rate-determining step in carbide mechanism. In contrast, the rate-determining step in oxygenate mechanism consists of acidic CO–$H_2$ complex that may be affected by surface basicity of catalyst. These changes in rate constant ($k$) with catalyst surface basicity enhance the presence of acidic compounds in rate-determining step as considered in oxygenate mechanism in comparison with carbide mechanism in total reaction. This kinetic results emphasis that the popular carbide mechanism cannot explain the FTS reaction on iron catalyst in details and has to be corrected.

Recently, Davis (2009) used the $^{14}C$-labled compound during FTS reaction with same approach that Emmet et al. was using. He explains that the FTS reaction mechanism involves an initiation component that differs from the species that are responsible for chain propagation. Because the iron catalyst has WGS activity, they propose that the chain initiation species is similar, or the same, as the intermediate in the WGS reaction. It is, therefore, viewed that an oxygen containing structure that is, or resembles, a formate species can be formed from either CO or $CO_2$ and this is responsible for chain initiation (Scheme 3). The species responsible for chain propagation differs from the structure of the chain initiation species and is derived predominantly from CO. It is emphasized that the C–O bond of the initiation species is not broken prior to the addition of the CO to extend the growing chain by one more carbon.

Gaube and Klein (2008) proposed a novel hypothesis for FTS mechanism, which involves two independent pathways for hydrocarbon formation. First pathway is based on the polymerization methylene units and the second, based on the insertion and hydrogenation of carbon monoxide. This great variety of experiments presented by many authors supports without exception the hypothesis that two incompatible mechanisms are involved resting exclusively on $-CH_2$ and on CO insertion respectively.

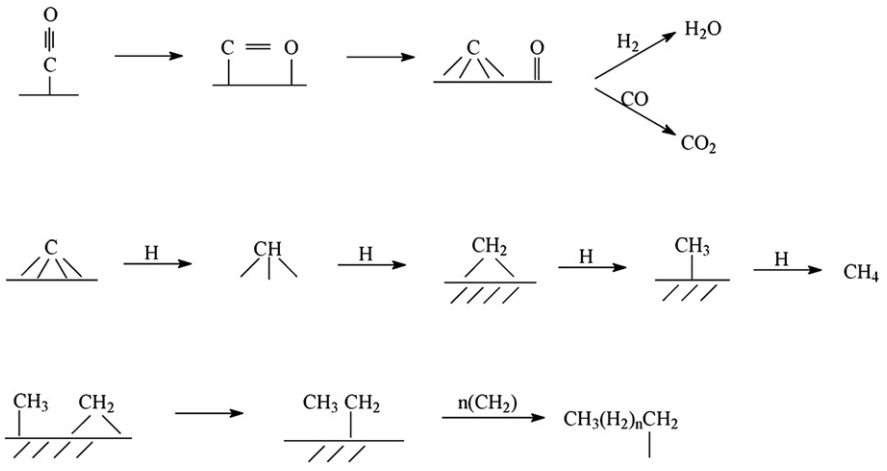


**Scheme 1.** (From Davis, 2009).

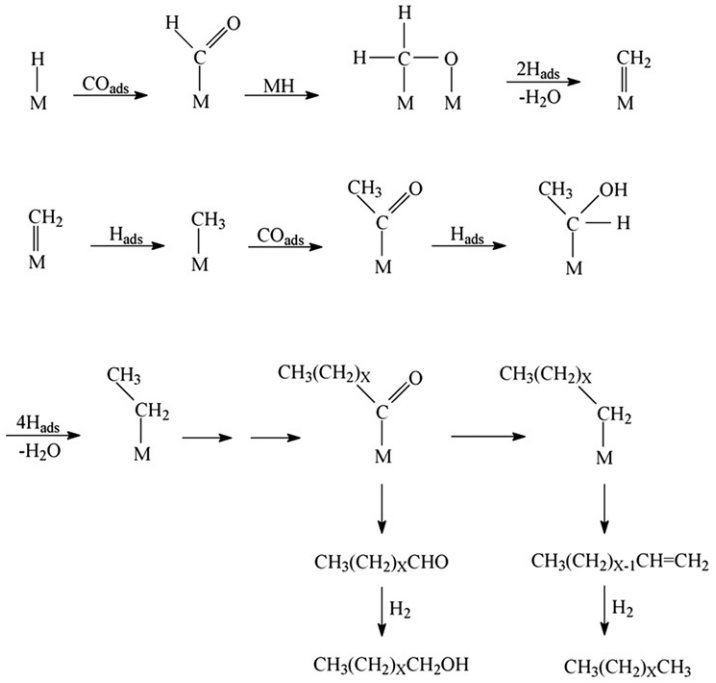

**Scheme 2.** (From Davis, 2009).

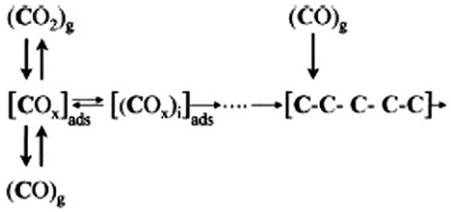

**Scheme 3.** (From Davis, 2009).

## 5. Conclusions

Promotion of nano-structured catalyst with Ca, Mg and La promoters has been shown significant influences on kinetic parameters contain rate constant ($k$) and adsorption parameter ($b$) in kinetic models proposed by Huff et al. (Huff and Satterfield, 1984). The addition of these promoters enhances the catalyst surface basicity in the order Ca > Mg > La and decreases the rate constant ($k$) for FTS reaction, which means that the FTS reaction rate was decreased with increasing the catalyst surface basicity.

In addition, the adsorption parameter ($b$) was decreased by increasing the catalyst surface basicity because of decreasing in the adsorption equilibrium constant of water and/or an increase in the adsorption of equilibrium constant of carbon monoxide leading to increase in the FTS reaction. These results show that raising the catalyst surface basicity has complicated effects on FTS reaction and an optimum promoter contains the rate constant ($k$), which is not very low and the adsorption parameter ($b$) is not extremely high.

## References


Anderson, R.B., 1956. Catalysts for the Fischer–Tropsch Synthesis, vol. 4. Van Nostrand Reinhold, New York.

Anderson, R.B., 1984. The Fischer–Tropsch Synthesis. Academic Press, Orlando, FL.

Arakawa, H., Bell, A.T., 1983. Ind. Eng. Chem. Proc. Des. Dev. 22, 97.

Bartholomew, C.H., 1991. Recent developments in Fischer–Tropsch catalysis. In: New Trends in CO Activation, Studies in Surface Science and Catalysis, vol. 64. Elsevier, Amsterdam.

Bell, A.T., 1981. Catal. Rev.-Sci. Eng. 23, 203.

Benziger, J., Madix, R., 1980. Surf. Sci. 94, 119.

Bukur, D.B., Lang, X., Nowiciki, L., 2001. Stud. Surf. Sci. Catal. 136, 165.

Davis, B.H., 2009. Catal. Today 141, 25.

Dictor, R.A., Bell, A.T., 1986. J Catal. 97, 121.

Dry, M.E., Shingles, T., Boshoff, L.J., Oosthuizen, G.J., 1969. J. Catal. 15, 190.

Dry, M.E., 1981. The Fischer–Tropsch synthesis. In: Anderson, J.R., Boudart, M. (Eds.), Catalysis- Science and Technology. Springer-Verlag, New York, p. 159.

Eriksson, S., Nylén, U., Rojas, S., Boutonnet, M., 2004. Appl. Catal. A 265, 207.

Fischer, F., Tropsch, H., 1926. Brennstoff-Chem. 7, 97.

Gallegos, N.G., Alvarez, A.M., Cagnoli, M.V., Bengoa, J.F., Marchetti, S.G., Mercader, R. C., Yeramian, A.A., 1996. J. Catal. 161, 132.

Gaube, J., Klein, H.-F., 2008. J. Mol. Catal. A: Chem. 283, 60.

Guczi, L., Lázár, K., 1991. Stud. Surf. Sci. Catal. 61, 251.

Hayashi, H., Chen, L.Z., Tago, T., Kishida, M., Wakabayashi, K., 2002. Appl. Catal. A 231, 81.

Herranz, T., Rojas, S., Pérez-Alonso, F.J., Ojeda, M., Terreros, P., Fierro, J.L.G., 2006. Appl. Catal. A 311, 66.

Hoc, W.N., Zhang, Y., O Brien, R.J., Luo, M., Davis, B.H., 2002. Appl. Catal. A: Gen 236, 77.

Huff Jr., G., Satterfield, C.N., 1984. Ind. Eng. Chem. Proc. Des. Dev. 23, 696.

Kummer, J.T., Browning, L.C., Emmett, P.H., 1948. J. Chem. Phys. 16, 739.

Li, X., Zhong, B., Peng, S., Wang, Q., 1994. Catal. Lett. 23, 245.

Li, S., Li, A., Krishnammorrthy, S., Iglesia, E., 2001. Catal. Lett. 77, 197.

Liu, C., Zou, B., Rondinone, A.J., Zhang, Z.J., 2000. J. Phys. Chem. B 104, 1141.

Luo, M., Davis, B.H., 2003. Appl. Catal. A: Gen 246, 171.

Mills, G.A., 1988. Catalysts for Fuels from Syngas, New Directions for Research, IEACR/090. IEA Coal Research, London. U.S. Nat. Tech. Info. Serv. No. IEARC 8901.

Nakhaei Pour, A., Zamani, Y., Tavasoli, A., Shahri, S.M.K., Taheri, S.A., 2008a. Fuel 87, 2004.

Nakhaei Pour, A., Shahri, S.M.K., Bozorgzadeh, H.R., Zamani, Y., Tavasoli, A., Marvast, M.A., 2008b. Appl. Catal. A: Gen 348, 201.

Nakhaei Pour, A., Shahri, S.M.K., Zamani, Y., Irani, M., Tehrani, S., 2008c. J. Nat. Gas. Chem. 17, 242.

Nakhaei Pour, A., Taghipoor, S., Shekarriz, M., Shahri, S.M.K., Zamani, Y., 2009. J. Nanosci. Nanotechnol. 9, 4425.

Nakhaei Pour, A, Housaindokht, M.R., Tayyari, S.F., Zarkesh, J. J. Nat. Gas. Chem., in press.

Podgurski, H.H., Kummer, J.T., DeWitt, T.W., Emmett, P.H., Am, J., 1950. Chem. Soc. 72, 5382.

Raje, A.P., O Brien, R.J., Davis, B.H., 1998. J. Catal. 180, 36.

Schwuger, M.J., Stickdorn, K., Schomacker, R., 1995. Chem. Rev. 95, 849–864.

Storch, H.H., Golumbic, N., Anderson, R.B., 1951. The Fischer–Tropsch and Related Synthesis. John Wiley & Sons, New York.

Tao, Z., Yang, Y., Zhang, C., Li, T., Wang, J., Wan, H., Xiang, H., Li, Y.W., 2006. Catal. Comm 7, 1061.
Van der Laan, G.P., Beenackers, A.A.C.M., 1999. Catal. Rev.-Sci. Eng. 41, 255.
Vannice, A., 1976. Catal. Rev.-Sci. Eng. 14, 153.
Yang, Y., Xiang, H.W., Xu, Y.Y., Bai, L., Li, Y.W., 2004. Appl. Catal. A: Gen 266, 181.
Yang, J., Sun, Y., Tang, Y., Liu, Y., Wang, H., Tian, L., Wang, H., Zhang, Z., Xiang, H., Li, Y. W., 2006. J. Mol. Catal. A: Chem. 245, 26.
Zhang, C.H., Yang, Y., Teng, B.T., Li, T.Z., Zheng, H.Y., Xiang, H.W., Li, Y.W., 2006. J. Catal 237, 405.
Zimmerman, W.H., Bukur, D.B., 1990. Can. J. Chem. Eng. 68, 292.